Plan B for particle physics: finding long lived particles at CERN

Bondarenko, K.

Author: Bondarenko, K.
Title: Plan B for particle physics: finding long lived particles at CERN
Issue Date: 2018-11-15

Chapter 5

Sensitivity of the SHiP and MATHUSLA experiments

5.1 Analytical estimates

A number of experiments have been proposed in recent years in order to probe for light, long-lived particles [110–116, 250]. The searches for such particles are also included in the scientific programs of existing experiments [106, 107, 251].

Although the LHC experiment is the flagship of the *Energy Frontier* exploration, its increased luminosity in the current and future runs mean that huge numbers of heavy flavored mesons and vector bosons are being created. This opens up the possibility to supplement the High Luminosity phase of the LHC with companion experiments. Several such experiments have been proposed: CODEX-b [112], MATHUSLA [113, 114] and FASER [115, 116].

Given that all these experiments can probe similar parameter spaces it is important to be able to assess their scientific reach uniformly, with clearly specified and identical assumptions. While Monte-Carlo simulations of both production and decay, complemented with background studies, will eventually offer the ultimate sensitivity curve for each of these experiments, it is crucial to have a sufficiently simple and fully controlled analytical estimate first. Such an estimate uncovers the main factors that influence the sensitivity. This permits us to scan over different models and experiment designs in a quick and efficient manner.

As it turns out, the ratios between the sensitivities of the experiments to a great extent do not depend on the specific model of the particle candidate, and are determined mainly by the geometry and the collision energies of the experiments, which allow for a comparison in a largely model-independent way. To illustrate this point we compare the potential of two proposed experiments: SHiP and MATHUSLA (see Sections 4.1, 4.2) [213]. We analyze their sensitivity to the scalar and neutrino portals, described in Chapters 2 and 3. In both models, for particle masses $M_X \lesssim$

m_{B_c} the main production channel is the decay of heavy flavored mesons.[1] This explains why both of them can be studied at the same time. We concentrate on the mass range $M_X \gtrsim m_K$ since the domain of lower masses for the HNL and Higgs-like scalar is expected to be probed by the currently running NA62 experiment [109, 251].

The sensitivity of the experiment is determined by the number of events one expects in the detector for a given value of each of the parameters. In realistic experiments such events need to be disentangled from the "background" signals.

For the SHiP experiment, detailed simulations have shown that one expects the number of background events to be very low, so that the experiment is "background free" [111, 244, 252, 253]. For the MATHUSLA experiment the background is also expected to be low [247] although no detailed studies have been performed yet. Even assuming the most favorable case of $N_{\rm bg} \ll 1$ one needs *on average* $\bar{N}_{\rm events} = 2.3$ expected signal events to observe at least one event with the probability higher than 90%.[2]

For both experiments considered here, the point of production is separated from the decay volume by some macroscopic distance $l_{\text{target-det}}$. For such experiments, the sensitivity curve has a typical "cigar-like shape" in the plane "mass vs. interaction strength". The *upper boundary* is determined by the condition that the decay length of a produced particle becomes comparable to the distance to the detector, $l_{\rm decay} \sim l_{\text{target-detector}}$. The *lower boundary* of the sensitivity region is determined by the parameters at which decays become too rare (i.e. $l_{\rm decay} \gg l_{\rm det}$). The intersection of these bounds defines the *maximal mass* which can be probed at the experiment.

The number of decay events in the detector factorizes into

$$N_{\rm events} = N_{\rm prod} \times P_{\rm decay} \tag{5.1.1}$$

where $N_{\rm prod}$ is the number of produced particles X. In the mass range $m_K \lesssim M_X \lesssim m_B$ the main production channels in proton-proton collisions for both HNLs and Higgs portal scalars are decays of heavy flavor mesons, see Sections 2.2 and 3.1 for discussion.[3] Therefore the number of produced feebly interacting particles $N_{\rm prod}$ is given by

$$N_{\rm prod} \approx \sum_{q,\text{meson}} \overbrace{2N_{q\bar{q}} \times f_{q\to\text{meson}}}^{N_{\rm meson}} \underset{\text{meson}\to X}{\mathrm{BR}} \times \epsilon_{\rm decay} \tag{5.1.2}$$

Here $N_{\bar{q}q}$ is the number of quark pairs produced; $f_{q\to\text{meson}}$ is the fraction of quark pairs that hadronise into a meson of a given type (such that the product of the two gives the number of mesons of a given type); $\mathrm{BR}_{\text{meson}\to X}$ is the branching of

[1] A significant part of the analysis is the same for neutrino and scalar models, so we denote the new particle by X.

[2] To obtain the 95% confidence limit one should assume $\bar{N}_{\rm events} = 3$, as the Poisson probability to see *at least one* event, while expecting 3 "on average" is $0.899\ldots$.

[3] We denote by $m_{\ldots}$ masses of lightest flavor mesons: kaons (m_K), D^+ (m_D) and B^+ (m_B).

the meson decay into X. Finally, $\epsilon_{\rm decay}$ is the *decay acceptance* – the fraction of particles X whose trajectory intersects the decay volume (i.e. particles that could decay inside).

The probability of decay into a state that can be detected is given by

$$P_{\rm decay} = \left[\exp\left(-\frac{l_{\text{target-det}}}{l_{\rm decay}}\right) - \exp\left(-\frac{l_{\text{target-det}} + l_{\rm det}}{l_{\rm decay}}\right)\right] \times \epsilon_{\rm det} \times \mathrm{BR}_{\rm vis} \qquad (5.1.3)$$

Here $l_{\text{target-det}}$ is the distance between the target and the entrance into the detector (see Sections 4.1, 4.2). For the purpose of presentation, in (5.1.3) we ignored the fact that particles travel slightly different distances, depending on their off-axis angle. The decay length $l_{\rm decay}$ in Eq. (5.1.3) is defined as

$$l_{\rm decay} = c\tau_X \beta\gamma \qquad (5.1.4)$$

where τ_X is the particle X's lifetime, $c\beta$ is its speed and γ is the Lorentz gamma-factor. Larger values of the γ-factor suppress the decay probability. This affects the upper and lower regions of the cigar-like sensitivity plots in the opposite fashions. For the lower limit, an experiment with the lower γ-factor is sensitive to the small coupling constants as we will see from Eq. (5.1.5). For sufficiently large couplings, having a larger γ-factor ensures that particles do not decay before reaching the detector, thus increasing the sensitivity to the upper range of the sensitivity curve.

The branching ratio $\mathrm{BR}_{\rm vis}$ is the fraction of all decays that produce final states that can be detected. Finally, $\epsilon_{\rm det} \leq 1$ is the *detection acceptance* – the fraction of all decays inside the decay volume for which the decay products could be registered.

5.1.1 Sensitivity comparison: main factors

For both neutrino and scalar portal, a single production channel dominates for each particular M_X. In this case, one can compare the sensitivity of two experiments without using specific branching ratio of particle production.

Let us first compare the lower boundary of the sensitivity region, where $l_{\rm decay} \gg l_{\rm det}$ and the decays are rare:

$$\frac{N_{\rm decay}^{SHiP}}{N_{\rm decay}^{\rm MAT}} \simeq \frac{N_{\rm meson}^{SHiP}}{N_{\rm meson}^{\rm MAT}} \times \frac{l_{\rm det}^{SHiP}}{l_{\rm det}^{\rm MAT}} \times \frac{\langle \gamma_{\rm meson}^{\rm MAT} \rangle}{\langle \gamma_{\rm meson}^{SHiP} \rangle} \times \frac{\epsilon_{SHiP}}{\epsilon_{\rm MAT}} \qquad (5.1.5)$$

The particles are assumed relativistic (we will see below when this assumption is justified) and the Lorentz-factor $\gamma_X \gg 1$ is estimated as

$$\langle \gamma_X \rangle \approx \frac{\langle E_{X,\text{meson frame}} \rangle}{M_X} \langle \gamma_{\rm meson} \rangle, \qquad (5.1.6)$$

where $\langle E_{X,\text{meson frame}} \rangle$ is the average energy of the particle X in the meson rest frame.

Experiment	N_D	$\langle\gamma\rangle_D$	N_B	$\langle\gamma\rangle_B$	$\langle l_{\rm det}\rangle$, m
MATHUSLA	3.6×10^{14}	2.6	2.6×10^{13}	2.3	38
SHiP	7.8×10^{17}	19.2	5.4×10^{13}	16.6	50

Table 5.1: Main numbers for the SHiP and MATHUSLA experiments. The total number of all D and B mesons (*not including antiparticles*) is reported for both experiments. For SHiP the numbers of mesons and γ-factors are based on Monte Carlo simulations [111], including enhancement due to the cascade production [246], for MATHUSLA the numbers are based on the FONLL simulations in order to include low p_T mesons (see text for details). The estimates assume $T_{SHiP} = 5$ years of running for SHiP and the integrated luminosity of $\mathcal{L}_h = 3000$ fb^{-1} for HL-LHC, relevant for MATHUSLA.

The relevant parameters for the MATHUSLA and SHiP experiments are summarized in Table 5.1 (see next Section for details).

5.1.2 Number and momentum distributions of mesons

In this Section, we estimate the number of mesons of a given type and their average γ-factor. For HNLs with masses $M_N \lesssim m_{D_s}$ 2-body decays of D_s provide dominant contribution (see e.g. Sec. 3.1), while for scalars the production from D mesons is negligible as compared to B-meson decays even for masses $m_K \lesssim M_S \lesssim m_D$ (see Sec. 2.2).

For the SHiP experiment, the production of charmed and beauty mesons were studied in detailed Pythia simulations, and the corresponding numbers can be found in the SHiP Technical proposal [111] and reproduced in Table 5.1. At the LHC production of heavy flavor mesons has been studied in both Run I and Run II (c.f. [254, 255]). However, in order to estimate the number of mesons for the MATHUSLA experiment, $N^{\rm MAT}_{\rm meson}$, one needs to know the meson p_T distribution in the MATHUSLA angular range, Table 4.3. The relevant distributions were measured for B^+ mesons by the CMS collaboration [255] (13 TeV) with the p_T cut $p_T^B \geqslant 10$ GeV, and for D^+/D_0 mesons by the ATLAS collaboration [254] (7 TeV) for$p_T^D \geqslant 3.5$ GeV (measurements performed by the LHCb collaboration [256–258] are performed in the forward rapidity range and therefore are not directly relevant for the MATHUSLA experiment). The low-p_T mesons, unaccounted in these studies, are the most relevant for the MATHUSLA sensitivity estimate for two reasons. Firstly, the spectrum of mesons produced in pp collisions has the form $d\sigma/dp_T \propto p_T^{-n}$ [259] for p_T above few GeV. This increases the number of D or B mesons as compared to those that passed the LHC cuts. Secondly, low-p_T mesons have the smallest γ-factor and therefore the shortest decay length (5.1.4) and the largest probability to decay inside the detector.

In order to evaluate the number of heavy flavor mesons at low p_T (and to estimate the D-meson production for $\sqrt{s} = 13$ TeV) we use the FONLL program [248, 249, 260, 261]. The FONLL predictions have been calibrated against the accelerator

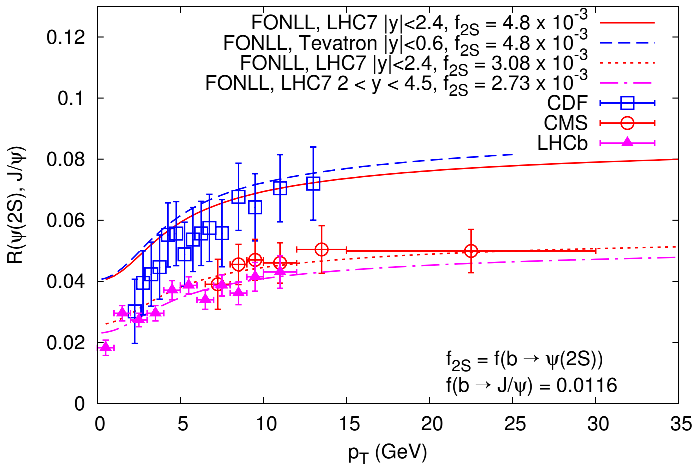

Figure 5.1: FONLL prediction of the ratio of the cross-section for non-prompt (i.e. from b-hadrons) production of $\psi(2S)$ and J/ψ as a function of their transverse momentum, compared to the experimental data from CDF at the Tevatron and CMS and LHCb at the LHC (the figure is reproduced from [260]).

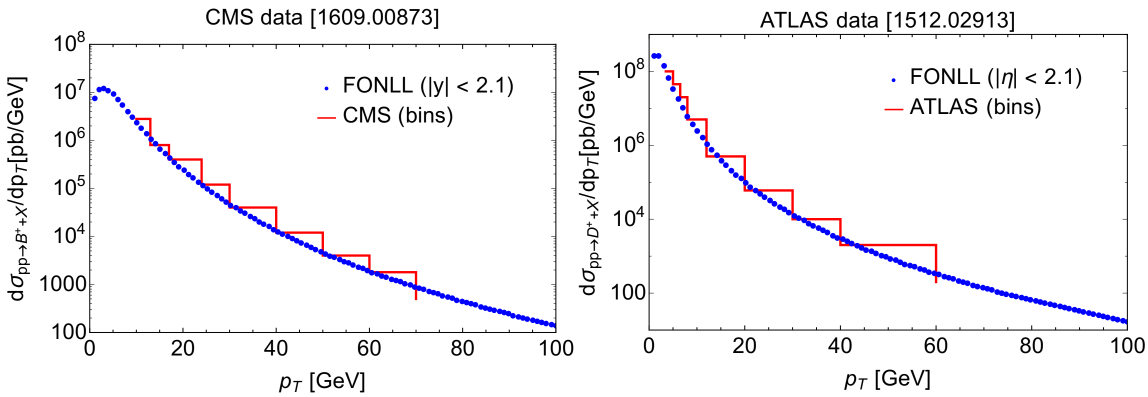

Figure 5.2: Comparison of the $p_T|$ spectrum of B^+, D^+ mesons as simulated by FONLL with the measurements by ATLAS and CMS experiments. Only the central values of the FONLL predictions are shown. See text for details.

data and were found to be in very good agreement, see e.g.[13, 254, 255, 257, 262]. In particular, by comparing the FONLL predictions with the Tevatron and LHC measurements of B^+ production, we see that FONLL predicts low-p_T distribution accurately, see Fig. 5.1. We provide the central value of the FONLL predictions down to $p_T = 0$, confronted with the measurements of the CMS [255] and ATLAS [254] collaborations in Fig. 5.2. As expected, the distributions have maxima, after which they fall down. The position of the maximum affects the total number of produced mesons N_{meson} and the average meson momentum $\langle|\mathbf{p}|\rangle_M$. Decreasing the position of the maximum by x changes the estimate of the decay events by x^2 which makes the accurate prediction of this number very important.

Using the results of FONLL simulations we find the number of low p_T mesons travelling in the MATHUSLA direction

$$\frac{N_D|_{p_T<3.5\text{ GeV}}}{N_D|_{p_T>3.5\text{ GeV}}} = 3.8, \quad \frac{N_B|_{p_T<10\text{ GeV}}}{N_B|_{p_T>10\text{ GeV}}} = 5.7 \tag{5.1.7}$$

At masses $M_X \gtrsim 3$ GeV the contribution of B_c meson decays may become important, depending on the production fraction $f(b \to B_c)$ (see Sec. 3.1.1.3). The production fraction of B_c mesons have been measured at the LHCb [223], and found to be in the range $f(b \to B_c) \simeq 2.6 \times 10^{-3}$. Earlier measurements at Tevatron have found a similar value $f(b \to B_c) \simeq 2 \times 10^{-3}$ [263–265]. For SHiP the corresponding production fraction at $\sqrt{s} \sim 30\,\text{GeV}$ is not known and therefore we perform our analysis for two extreme cases: *(i)* $f(b \to B_c)$ at SHiP the same as at the LHC and *(ii)* "no B_c mesons".

To evaluate the pseudo-rapidity and p_T distributions of B_c mesons we compared the results of BCVEGPY 2.0 package [266] (that simulates the distribution of B_c mesons and was tested at the LHC energies) with that of FONLL for B^+ mesons. We conclude that p_T and η distributions of B_c and B^+ have similar shapes. Therefore we used the appropriately rescaled distributions of B^+ mesons in order to estimate the B_c contribution for the SHiP experiment.

The numbers for both experiments are summarized in Table 5.1. One sees that the number of charmed mesons is much larger at SHiP, the numbers of B mesons are comparable between the experiments and the average mesons momenta (and therefore γ-factors) are lower at MATHUSLA. This is caused by their different geometric orientation relative to the proton beams directions: SHiP is located in the forward direction, while MATHUSLA is about 20° off-axis.

5.1.3 Shape of the sensitivity curve

5.1.3.1 Upper bound of the sensitivity curve

Let us now discuss the upper bound of the sensitivity curve, the value of U^2 that we call U^2_{top}. For simplicity, we will concentrate on the HNL case and later will comment on small differences that arise in the scalar case.

The dependence of the decay probability (5.1.3) on the mixing angle is such that for a fixed mass M_N the number of decay events increases as U^4, then reaches the maximum and falls exponentially (see Fig. 5.3, left). The mixing angle for which the amount of detected HNLs is maximal $U_{\max}(M_N)$ could be estimated from the condition that the HNL decay width is equal to the distance from the target to the detector

$$l_{\text{decay}}(M_N, U^2_{\max}(M_N)) \simeq l_{\text{target-det}} \tag{5.1.8}$$

The HNL mass dependence of $U_{\max}$ is shown on Fig. 5.3, right.

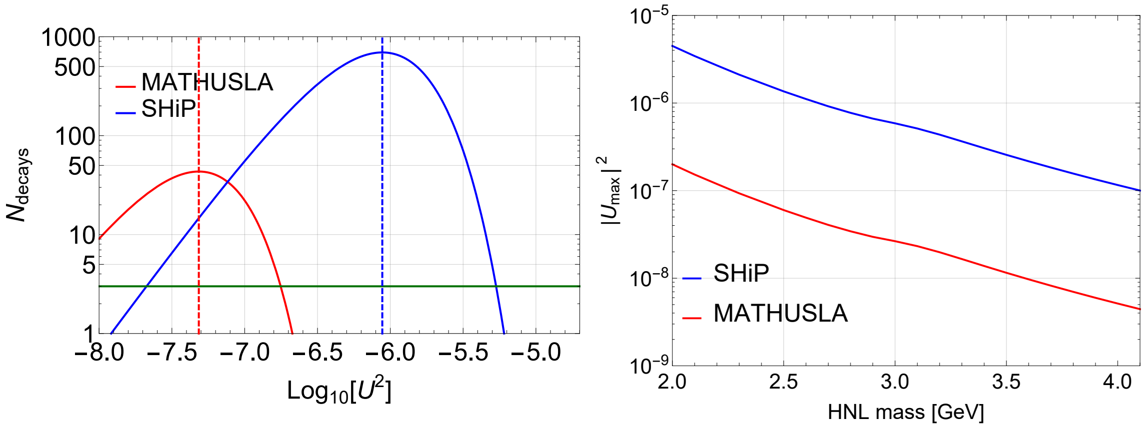

Figure 5.3: Left: the number of HNL decays events as a function of coupling $|U|^2$ for $M_N = 3$ GeV at SHiP and MATHUSLA experiments; green horizontal line denotes 3 decay events, while dashed vertical line corresponds to $U_{\rm max}$. Right: values of $|U_{\rm max}|^2$ for the MATHUSLA and SHiP experiments. Note that $U_{\rm max}$ is not equal to the upper boundary of the sensitivity curve!

The upper bound of sensitivity, $U_{\rm top}$, appears when the exponential suppression due to the increasing probability to decay before reaching the detector outweighs the amount of produced HNLs. If all HNLs had the same energy, $\langle E_N \rangle$, then the upper bound of sensitivity would be given by $U^2_{\rm top}(M_N) \simeq U^2_{\rm max}(M_N) \times \log\left(N_{\rm prod}(M_N, U^2_{\rm max}(M_N))\right)$. The ratio R between $U^2_{\rm top}$ and $U^2_{\rm max}$ in this case is presented in Fig. 5.4 as dashed lines for two experiments.

However, for the correct estimation of $U_{\rm top}$ it is important to take into account the distribution of the HNLs by energy dN/dE_N. The upper bound will be determined by the high-energy tail of the distribution, as the decrease of $c\tau$ with the growth of U^2 can be compensated by the increase of γ-factor of the HNL that occur in decays of most energetic mesons. The resulting decay probability (5.1.3) is modified as

$$P_{\rm decay} \approx \int dE_N \frac{dN}{dE_N} e^{-l_{\text{target-det}}\Gamma_N M_N/E_N}. \tag{5.1.9}$$

The HNLs in question are produced from decays of B-mesons. The high-energy tail of B mesons distribution function at SHiP is well described by the exponential distribution, see the left Fig. 5.5.

$$\frac{dN}{dE_B} = f_0 e^{-E_B\delta}, \quad \delta \approx 2.5\cdot 10^{-2}\ \text{GeV}^{-1} \quad \text{and} \quad f_0 \approx 0.1\ \text{GeV}^{-1} \tag{5.1.10}$$

The distribution of B-mesons in MATHUSLA experiment for $E_B \lesssim 300$ GeV can be approximated by the power law function, see the right Fig. 5.5:

$$\frac{dN}{dE_B} \approx \tilde{f}_0 E_B^{-\alpha}, \quad \tilde{f}_0 \approx 1.6\cdot 10^4\ \text{GeV}^{\alpha-1}, \quad \alpha \simeq 4.6 \tag{5.1.11}$$

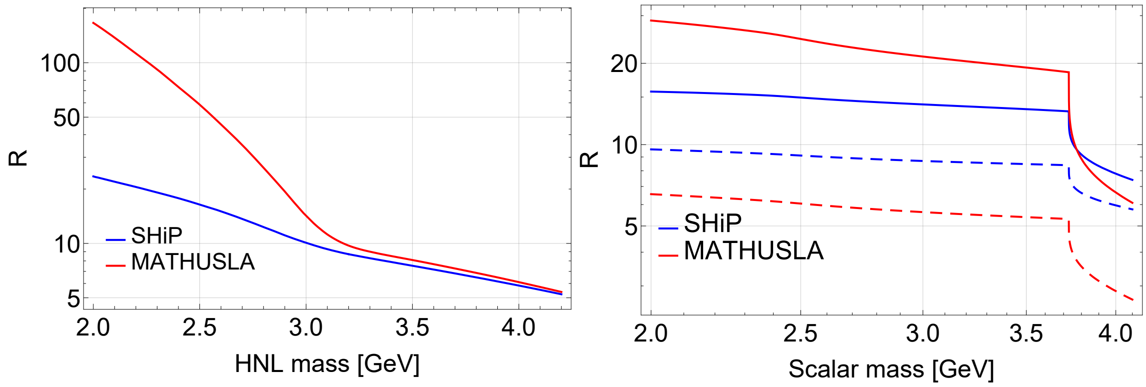

Figure 5.4: Ratios $R = U^2_{\text{top}}/U^2_{\text{max}}$ for HNLs mixing with ν_e (left) and for scalars (right) at SHiP and MATHUSLA experiments. Dashed lines are obtained under the assumption that all particles have the same average energy and neglecting the energy distribution tails.

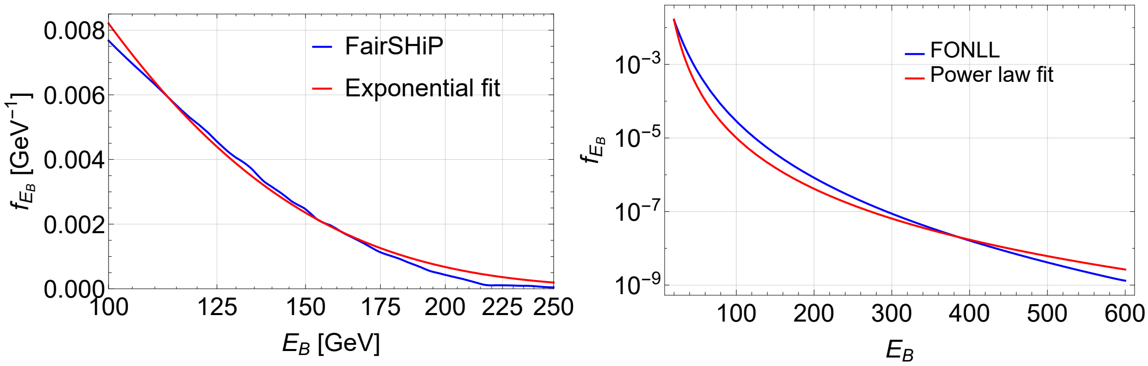

Figure 5.5: Fits of the high energy B mesons distribution function at SHiP (data taken from [246]), left, and at MATHUSLA (provided by FONLL), right

Using the distributions (5.1.10)–(5.1.11) and relation between the energy of the parent B-meson and daughter HNL, we can improve the estimates of the upper sensitivity bound (see details in the Appendix F). The corresponding ratios $R = U^2_{\text{top}}/U^2_{\text{max}}$ for SHiP and MATHUSLA are given in Fig. 5.4. For SHiP the dependence of R on the HNL mass is logarithmic, while for MATHUSLA it is a power law.

Finally, we comment on the difference between the HNL and scalar cases. The decay width Γ_S changes with mass slower than Γ_N, see the discussion in Sec. 5.1.3.2. In addition, $\text{Br}_{B\to S+X}$ behaves with mass monotonically, while for HNLs new production channels appear at different masses. Therefore the upper bound width for scalars changes with mass less than for HNLs.

5.1.3.2 Maximal probed mass

The maximal mass probed by the experiment is defined as the mass at which the lower sensitivity bound (decays are very rare) meets the upper sensitivity bound (particles decay before reaching the detector). It can be roughly estimated from the relation

$$l_{\text{target-det}} \lesssim l_{\text{decay}} \tag{5.1.12}$$

where for the models in question

$$l_{\text{decay}} \simeq \frac{\langle E\rangle}{M_X} \times \begin{cases} 170\,\text{cm}\left(\frac{10^{-5}}{U^2}\right)\left(\frac{2\,\text{GeV}}{M_X}\right)^5, & \text{HNL. Mixing with } U_{e/\mu} \text{ only} \\ 454\,\text{cm}\left(\frac{10^{-5}}{U_\tau^2}\right)\left(\frac{2\,\text{GeV}}{M_X}\right)^5, & \text{HNL. Mixing with } U_\tau \text{ only} \\ 0.015\,\text{cm}\left(\frac{10^{-5}}{\sin^2\theta}\right)\left(\frac{2\,\text{GeV}}{M_X}\right)^2, & \text{scalar} \end{cases} \tag{5.1.13}$$

where $\langle E\rangle$ is the average energy of a particle X, M_X is the particle's mass and U^2 (correspondingly, $\sin^2\theta$) are dimensionless parameters that specify how much weaker is the parameter controlling the interaction of the particle X than the interaction of neutrino (correspondingly, Higgs boson), see Sections 2.3 and 3.2 for details.

The maximal mass can be found from Eq. (5.1.12) via

$$M_{X,\max} \propto \left(\frac{\langle E\rangle}{|\phi|^2_{\min} l_{\text{target-det}}}\right)^{1/(\alpha+1)} \tag{5.1.14}$$

where $\alpha = 2$ (correspondingly $\alpha = 5$) for the case of scalar (correspondingly, HNL) and $|\phi|^2 = |\phi|^2_{\min}$, is the value of parameter U^2 (or $\sin^2\theta$) that corresponds to $\bar{N}_{\text{events}}$ detected events for $M_X < M_{X,\max}$.

For the ratio of the maximally probed masses at SHiP and MATHUSLA, we obtain

$$\frac{M^{SHiP}_{X,\max}}{M^{\text{MAT}}_{X,\max}} \approx \left(\frac{\langle E\rangle^{SHiP}}{\langle E\rangle^{\text{MAT}}} \times \frac{|\phi|^{2,\text{MAT}}_{\min}}{|\phi|^{2,SHiP}_{\min}} \times \frac{l^{\text{MAT}}_{\text{tar-det}}}{l^{SHiP}_{\text{tar-det}}}\right)^{1/(\alpha+1)} \tag{5.1.15}$$

This estimation is valid for the masses M_X not too close to the production threshold, which corresponds to masses $M_X = m_B - m_K$ for scalars and $M_X = m_B$ for HNLs.

5.1.4 Results

Our results are summarized in Fig. 5.6 for HNLs mixed with light (electron) and heavy (τ) flavors. In Fig. 5.7 we show the sensitivity of both experiments to the scalar.

Qualitatively, for particles produced in B-meson decays (HNLs with masses $M_N > m_D$ and scalars with masses $M_S > m_K$) MATHUSLA can probe factor $\sim 2-3$ smaller mixing angles (U^2 or $\sin^2\theta$) than SHiP. This conclusion holds *assuming* no background events for both experiments and *similar detection efficiency*. For the HNLs in the mass range $m_K \lesssim M_N \lesssim m_D$ the smaller γ-factor of MATHUSLA

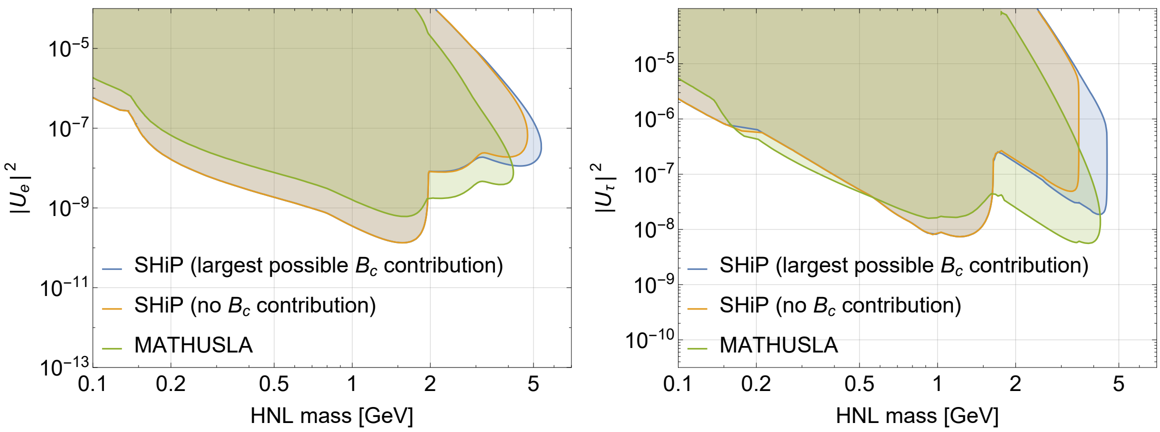

Figure 5.6: Comparison of sensitivity for SHiP and MATHUSLA for HNL models. The production fraction of B_c mesons at SHiP is not known, so we take the largest possible contribution of B_c based on the production fraction measured at the LHC, $f(b \to B_c) = 2.6 \times 10^{-3}$. In case of the SHiP experiment we take into account proper geometrical acceptance (calibrated against the Monte-Carlo simulations [212] and select only those channels where at least two charged tracks from the HNL decay appear. In the case of the MATHUSLA experiment we optimistically used both decay and detection acceptances equal to 100%.

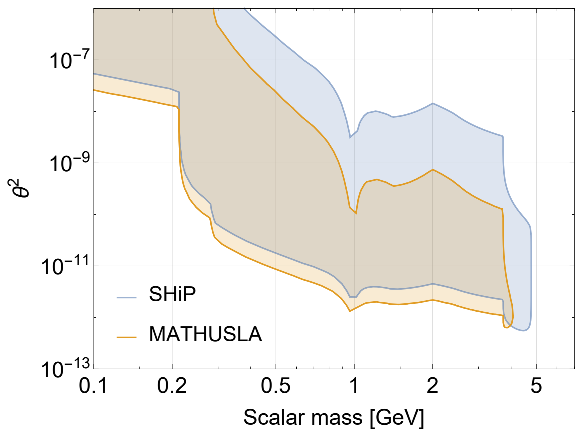

Figure 5.7: Comparison of sensitivities of SHiP and MATHUSLA experiments for the scalar portal model. In case of the SHiP experiment, we took into account proper geometrical acceptance (calibrated against the Monte-Carlo simulations [267] and also selected only those channels where at least two charged tracks from the HNL decay appear. In case of MATHUSLA experiment we optimistically used both decay and detection acceptances equal to 100%.

does not compensate 3 orders of magnitude difference in the number of D mesons (see Table 5.1) and therefore the SHiP reaches about 1 order of magnitude lower in sensitivity for U^2. The comparison between the number of events is

$$\left.\frac{N^{N,SHiP}_{\text{decay}}}{N^{N,\text{MAT}}_{\text{decay}}}\right|_{M_N\lesssim m_D} \simeq 127, \quad \left.\frac{N^{N,SHiP}_{\text{decay}}}{N^{N,\text{MAT}}_{\text{decay}}}\right|_{M_N\gtrsim m_D} \simeq \left.\frac{N^{S,SHiP}_{\text{decay}}}{N^{S,\text{MAT}}_{\text{decay}}}\right|_{M_S\gtrsim m_K} \simeq \frac{1}{7.6} \tag{5.1.16}$$

The smaller γ-factor of MATHUSLA adversely affects the maximal mass that can be probed (as well as the upper bound of the sensitivity curves). The maximally probed masses ratios (5.1.15) are

$$\text{HNL:} \quad \frac{M^{N,SHiP}_{\text{max}}}{M^{N,\text{MAT}}_{\text{max}}} \approx 1.7, \qquad \text{Scalar:} \quad \frac{M^{S,SHiP}_{\text{max}}}{M^{S,\text{MAT}}_{\text{max}}} \approx 2.2 \tag{5.1.17}$$

5.2 Monte Carlo-based sensitivity estimates

The sensitivity estimates depend on the geometric acceptance. The latter is a function of particle's mass and in the case of the HNL, also the function of the mixing type. In order to evaluate the acceptance we compared our results with the `FairSHiP` simulations [212, 267]. `FairSHiP` is a `FairRoot`-based [268] Monte Carlo software framework developed by the SHiP collaboration. In the simulation, fixed-target collisions of protons are generated by `Pythia 8` [269], neutrino interactions by `GENIE` [270] and inelastic muon interactions by `Pythia 6` [271]. Secondary heavy flavor production in cascade interactions of hadrons originated by the initial proton collision [246] is also taken into account, which leads to the increase of the overall production fraction, taken into account in Table 5.1. The SHiP detector response is simulated with the `GEANT4` [272]; the SHiP spectrometer tracking stations are described in [273] and the particle identification tools are presented in [274].

5.2.1 FairSHiP: simulation framework for the SHiP experiment

The experimental sensitivity to HNLs was previously explored for several benchmark models [111, 252] assuming particular ratio between the three HNL mixing angles [129, 218]. The current study updates the previous results in a number of important ways. Recent work [275] revised branching ratios of HNL production and decay channels and evaluated several new channels not considered before. In addition, the estimates of the number of D- and B-mesons now include cascade production [246]. We further add an evaluation of the SHiP sensitivity limit for large values of the mixing angles U^2. In addition, our current sensitivity estimates are not limited to a set of benchmark models. Instead, we provide a model-independent way to compute the sensitivity for *any* model ratio of mixing angles.

A single `FairShip` simulation takes the HNL mass, M_N, and its couplings to the Standard Model flavors U_e, U_μ, U_τ as input parameters. The mass dependent branching ratios (based on [275], see Sec. 3.1) for leptonic and semileptonic decays of charm and beauty mesons, τ leptons, etc to HNL, are made available to `Pythia`

pp cross-section	$\bar{c}c$ fraction	$\bar{b}b$ fraction	Cascade enhancement f_{cascade}	
σ_{pp}	$X_{\bar{c}c}$ [276]	$X_{\bar{b}b}$ [277]	charm [246]	beauty [246]
10.7 mb	1.7×10^{-3}	1.6×10^{-7}	2.3	1.7

Table 5.2: Charm and beauty production values. Total number of mesons of a given flavor is defined by $N_q = 2 \times X_{\bar{q}q} \times f_{\text{cascade}} \times N_{\text{PoT}}$. The number of protons on target over 5 years of the experiment's run is $N_{\text{PoT}} = 2 \times 10^{20}$.

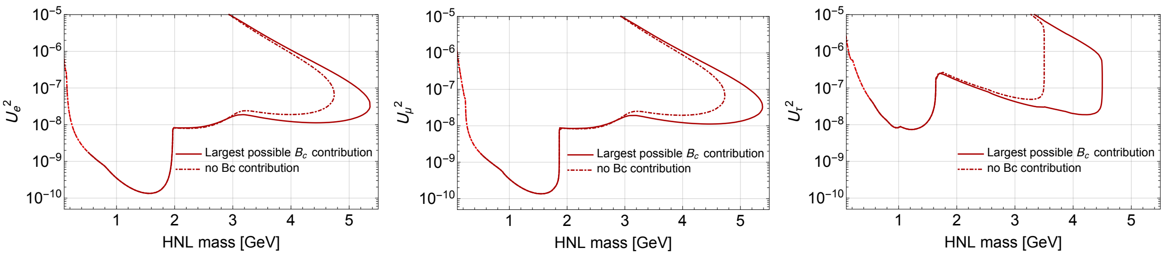

Figure 5.8: SHiP sensitivity curves (90%CL) for mixing with a single flavor: U_e (left), U_μ (middle), U_τ (right). Dashed-dotted line: contribution from B_c mesons not included; solid line: contribution of B_c mesons is included with the production fraction equal to that at the LHC energies: $f(b \to B_c) = 2.6 \times 10^{-3}$. The region between two curves shows a range of potential contribution from B_c depending on its actual production fraction. Below m_K only contributions from D-mesons have been included (dashed lines).

8. A registered "decay event" in the detector requires two charged tracks that also satisfy a number of selection criteria as described in [274].

For HNLs with masses $M_N \lesssim 500$ MeV, kaon decays provide the dominant production channel. While $\mathcal{O}(10^{20})$ kaons are expected at SHiP, most of them scatter in the target and/or hadron stopper before decaying. A proper estimate of the number of kaons decaying into HNLs is not currently included in the `FairSHiP`. It is expected that NA62 experiment [107, 109, 251] will cover the region below kaon mass.

Detailed background studies have been performed for the SHiP experiment [111, 244, 252, 253]. They demonstrate that there is a negligible amount of background events after selection and veto cuts over the lifetime of the experiment. The experiment is essentially "background free" which greatly simplifies the analysis – it is sufficient to count the number of events for a given value of mixings. One therefore defines the *90% confidence region* as a region in the parameter space where one expect $\bar{N}_{\text{events}} = 2.3$ signal events *on average*.

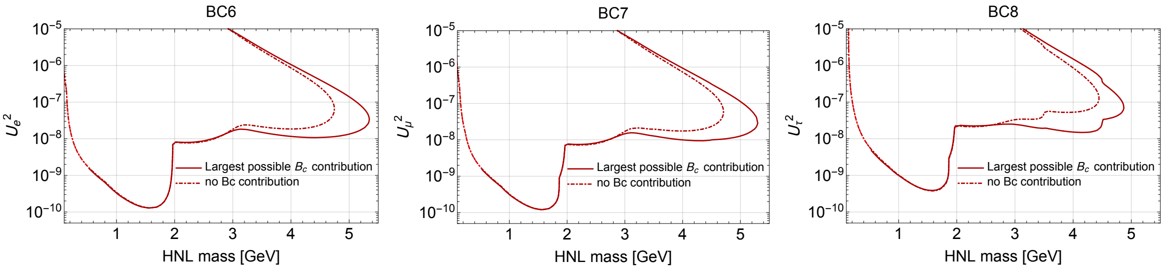

Figure 5.9: Sensitivity curves for 3 benchmark models, 90%CL (see text for details)

5.2.2 Sensitivity towards HNLs

5.2.2.1 Sensitivity for mixing with individual flavors and benchmark models

We present our results in several forms. Firstly, we present sensitivity curves (90% CL) for mixing with each individual flavor (Fig. 5.8). For masses above ~ 3 GeV, the contribution of B_c mesons to the HNL production can have an important (even dominant) role for the production fractions $f(b \to B_c)$ as low as 10^{-3} (see Sec. 3.1.1.3 for details). As the yield of B_c mesons at SHiP energies is not known, we provide two estimates. For the optimistic estimate $f(b \to B_c)$ is assumed at the LHC level 2.6×10^{-3} [223] while for the pessimistic estimate we do not include B_c mesons at all.

We also provide sensitivity estimates of three "benchmark models" used in the Technical proposal [111]. These models allow to explain the data of neutrino flavor oscillations while at the same time maximizing the mixing to a one particular flavor [129, 218]. They are

– **BC6:** $U_e^2 : U_\mu^2 : U_\tau^2 = 52 : 1 : 1$
– **BC7:** $U_e^2 : U_\mu^2 : U_\tau^2 = 1 : 16 : 3.8$
– **BC8:** $U_e^2 : U_\mu^2 : U_\tau^2 = 0.061 : 1 : 4.3$

The sensitivity curves for these models are shown in Fig. 5.9.

5.2.2.2 Full sensitivity matrix for HNLs at SHiP

We will demonstrate below that the lower limit of the sensitivity curve has a simple analytical dependence on the set of mixing angles $\overrightarrow{U^2} \equiv \{U_e^2, U_\mu^2, U_\tau^2\}$. This allows to extract all the relevant information about the lower limit of sensitivity for any model with just a handful of simulations.

Production of HNLs at SHiP proceeds via leptonic or semileptonic heavy flavor decays with other channels being irrelevant (c.f. [275]). The dependence on U_α^2 factors out and therefore the total number of produced HNLs is given by

$$N_{\text{prod}}(M_N|\overrightarrow{U^2}) = \sum_\alpha U_\alpha^2 N_\alpha \tag{5.2.1}$$

where N_α is the number of HNLs that would be produced through *all possible channels* with the mixings $U_\alpha = 1; U_{\beta\neq\alpha=0}$:

$$N_\alpha \equiv \sum_{\text{hadrons } h} N_h \left(\sum_{\text{channels}} \text{BR}_{h\to N+X_\alpha}\Big|_{U_\alpha=1;U_{\beta\neq\alpha=0}} \right) \tag{5.2.2}$$

Here N_h is the number of hadrons of a given type h; $\text{BR}_{h\to N+X_\alpha}$ is a branching ratio for their decay into an HNL plus any number of other particles (whose total flavor lepton number $L_\alpha = 1$). By its definition N_α depends on the HNL mass and flavor *type* only. To make notations compact we will sometimes rewrite Eq. (5.2.1) as

$$N_{\text{prod}} = \overrightarrow{U^2} \cdot \vec{N} \tag{5.2.3}$$

In the limit when the decay length is much larger than the distance to the detector (and of the detector size), the U_α^2 dependence also factorizes similarly to Eq. (5.2.1):

$$P_{\text{decay}}(M_N|\overrightarrow{U^2}) = \sum_\alpha U_\alpha^2 P_\alpha \tag{5.2.4}$$

The corresponding P_α is given by:

$$P_\alpha = \frac{l_{\text{det}}}{l_{\text{decay}}} \sum_X \text{BR}(N \to X_{\text{detectable}})\Big|_{U_\alpha=1;U_{\beta\neq\alpha=0}} \tag{5.2.5}$$

Here $l_{\text{decay}} = c\tau_N\gamma$ is the decay length of an HNL, l_{det} is the detector length (we assume that $l_{\text{decay}} \gg l_{\text{det}}$) and all quantities in the right hand side, including l_{decay}, are evaluated for $U_\alpha = 1; U_{\beta\neq\alpha} = 0$.

As a result, the number of detected events will be given by

$$N_{\text{decay}}\left[M_N|\overrightarrow{U^2}\right] = \sum_{\alpha,\beta} U_\alpha^2 \mathcal{M}_{\alpha\beta}(M_N) U_\beta^2 \tag{5.2.6}$$

where the matrix $M_{\alpha\beta}(M_N)$ is defined as

$$\mathcal{M}_{\alpha\beta} \equiv N_\alpha P_\beta \tag{5.2.7}$$

where N_α and P_α are defined via Eqs. (5.2.2) and (5.2.5) correspondingly. The matrix $M_{\alpha\beta}$ depends *only* on HNL's mass and *does not* depend on the mixing angles.

5.2.2.3 Procedure to determine the sensitivity matrix

To determine $M_{\alpha\beta}$ one needs to run 9 Monte Carlo simulations for each mass. Namely, one runs 3 simulations with vectors $\overrightarrow{U^2} = (x, 0, 0)$, $\overrightarrow{U^2} = (0, x, 0)$, $\overrightarrow{U^2} = (0, 0, x)$, where x is any sufficiently small number such that $l_{\text{decay}} \gg l_{\text{det}}$. Next one runs a set of 6 non-physical simulations, where a particle is produced solely via channel α and decays solely through the channel $\beta \neq \alpha$, thus providing non-diagonal matrix elements.

The resulting matrix has the form

$$\mathcal{M}_{\alpha\beta}\Big[M_N{=}1.5\,\mathrm{GeV}\Big] = 10^{20}\begin{pmatrix} 1.33 & 1.14 & 0.35 \\ 1.46 & 1.46 & 0.38 \\ 7.46\cdot 10^{-4} & 6.79\cdot 10^{-4} & 1.75\cdot 10^{-4}\end{pmatrix} \tag{5.2.8}$$

Knowing this matrix one can compute the sensitivity curve $U_\alpha(M)$ by solving the equation

$$\sum_{\alpha\beta} U_\alpha^2 \mathcal{M}_{\alpha\beta}(M_N) U_\beta^2 = N_{\text{events}} \tag{5.2.9}$$

By choosing different values of N_{events} one can obtain 90%, 95%, etc. confidence intervals or simply predict how many events one expects for a given vector of mixing angles $\overrightarrow{U^2}$. It should be stressed that only the *lower* limit of sensitivity can be assessed with such method (which is important for $M_N \gtrsim 2$ GeV).

For each mass we provide the results in the form

HNL Mass	$\mathcal{M}_{ee}$	$\mathcal{M}_{e\mu}$	$\mathcal{M}_{e\tau}$	$\mathcal{M}_{\mu e}$	$\mathcal{M}_{\mu\mu}$	$\mathcal{M}_{\mu\tau}$	$\mathcal{M}_{\tau e}$	$\mathcal{M}_{\tau\mu}$	$\mathcal{M}_{\tau\tau}$

The results are available at https://ship.web.cern.ch/ship/Sensitivity_Matrix/README that provides instructions for reading the file and generating sensitivity curves at different confidence levels.

5.2.3 Sensitivity towards dark scalars

SHiP sensitivity to the scalar portal discussed in the Sec. 5.1 was validated by FairShip simulation tool, see Fig. 5.10. We see that simulations are in good agreement with the analytical estimate.

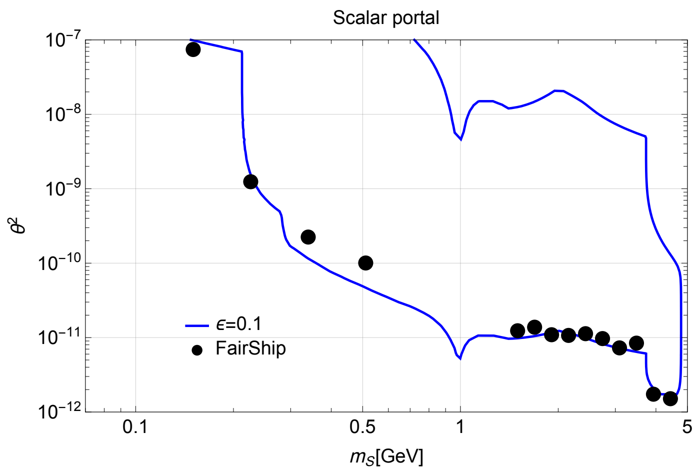

Figure 5.10: Comparison between analytical estimation of the SHiP sensitivity for acceptance $\epsilon = 0.1$ (blue line) with the results of the FairShip simulation (black points).